Received: 20 May 2019 | Revised: 12 June 2019 | Accepted: 17 June 2019

DOI: 10.1002/jmr.2804

RESEARCH ARTICLE

WILEY Journal of Molecular Recognition

Molecular toxicity of nanoplastics involving in oxidative stress and desoxyribonucleic acid damage

Tongtong Zheng[1] | Dong Yuan[3] | Chunguang Liu[1,2]

[1] School of Environmental Science and Engineering, Shandong Key Laboratory of Water Pollution Control and Resource Reuse, China–America CRC for Environment and Health of Shandong Province, Shandong University, Qingdao, China

[2] Guangdong Provincial Key Laboratory of Environmental Pollution and Health, School of Environment, Jinan University, Guangzhou, China

[3] Guangzhou Key Laboratory of Environmental Exposure and Health, School of Environment, Jinan University, Guangzhou, China

Correspondence
Chunguang Liu, School of Environmental Science and Engineering, Shandong Key Laboratory of Water Pollution Control and Resource Reuse, China–America CRC for Environment and Health of Shandong Province, Shandong University, 72# Jimo Binhai Road, Qingdao, Shandong 266237, China.
Email: chunguangliu2013@sdu.edu.cn

Funding information
China Postdoctoral Science Foundation funded project, Grant/Award Number: 2018M640631; The Fundamental Research Funds of Shandong University, Grant/Award Number: 2018JC059; Natural Science Foundation of Shandong Province, China, Grant/Award Number: ZR2019BB049; Guangzhou Key Laboratory of Environmental Exposure and Health, Grant/Award Number: GDKLEEH201805; National Natural Science Foundation of China, Grant/Award Number: 21507071

Abstract

Microplastic pollution attracted extensive attention because of its global presence and adverse effects on ecosystem. However, it is insufficient to clear the effects of nanoplastics on organisms at the molecular level. Herein, a nanopolystyrene (50 nm) was used to examine molecular responses of superoxide dismutase (SOD) and desoxyribonucleic acid (DNA) using spectroscopy (UV-vis, circular dichroism spectra, and fluorescence measurements) and single cell gel electrophoresis methods. Results showed that nanopolystyrene induced oxidative stress, involving in the increase of SOD activity and malondialdehide (MDA) content, and DNA damage because of the significant increase of olive tail moment, head optical density, and tail DNA percentage in the groups at exposure concentrations above 5×10^{-6} mol/L. The second structural and microenvironment of aromatic amino acids of SOD were changed with nanopolystyrene exposure. The fluorescence of SOD was quenched by nanopolystyrene at exposure concentration above 1×10^{-5} mol/L, and the quenching mode could be ascribed to the static type. The results and the combined methods are favorable to explore the molecular toxicity of other nanoplastics and the interaction mechanism.

KEYWORDS

comet assay, DNA damage, nanoplastics, spectral analysis, superoxide dismutase

1 | INTRODUCTION

Plastic debris in the environment is growing gradually due to the mass production of plastics and the discard without an effective processing.[1,2] These plastic debris in the environment gradually becomes millimeter plastics (microplastics [MPs]) and nanometer-scale plastics (nanoplastics [NPs]),[3] because of illumination radiation, wave shear hydrolysis, and microorganism action.[4,5] This change in size affects their environmental behavior such as migration, transformation, bioavailability, and toxicity.[6-8] For example, NP is more toxic than MP.[9] The adverse effects of MPs have been certified by research at cellular and organism level,[10-13] which includes but not limits to mortality, energy disturbance, inhibited growth and development, endocrine disruption, and genotoxicity.[14,15] Most of the researches concludes that the mechanisms of the toxic effects of MPs/NPs involves oxidative stress and the formation of reactive oxygen species (ROS).[4,14] However, there is little information on the mechanism of MPs/NPs-induced oxidative stress at

molecular level, which is necessary to evaluate the biological effects of NPs.

Alterations of the antioxidant defense system is one of the reasons of oxidative stress, while change of structure and function of antioxidant enzymes can be an indication of the oxidative stress.[16,17] Superoxide dismutase (SOD) is a potent ROS-metabolizing enzyme that occurs in most organisms. It is responsible for maintaining the cellular redox state and protecting cells from oxidative damage.[18] Nasser and Lynch reported that proteins can interact with MPs/NPs to form "protein corona," resulting in the change of the environmental behavior and toxicity of NPs.[19] However, information is insufficient to clear the effects of the MPs/NPs on the physiological function of SOD. On the other hand, although MPs/NPs can bind or interact with desoxyribonucleic acid (DNA), information about its genotoxicity is still limited.[20] Therefore, nanopolystyrene (NPS) was chosen as a model of NP, because of the nondegradability and wide distribution in the environment, accounting for 24% of the macroplastics in the estuarine habitat.[11] Also, it was widely studied due to its cytotoxicity as medical material for the organ imaging, drug delivery, implants, and so on.[21]

The main aim of this study is to explore the conformational and functional changes of SOD induced by nano-NPS using spectroscopy methods (UV-vis, circular dichroism spectra, and fluorescence measurements) and DNA damage with comet assay, which can help us better understand the mechanism of NP-induced oxidative stress and genotoxicity at the molecular level.

2 | MATERIALS AND METHODS

2.1 | Material

SOD was obtained from Sigma (Shanghai, China). NPS (50 nm) and H_2O_2 was obtained from Aladdin Reagent (Shanghai, China). KH_2PO_4 and K_2HPO_4 (Tianjin Kermel Chemical Reagent Co, Ltd) were used to prepare buffer solution (Phosphate buffered saline [PBS], pH = 7.4). Normal melting agarose (NMA) and low melting agarose (LMA) were purchased from Biowest, Spain. All reagents (analytical grade) were prepared with ultrapure water (18.25 Ω). Rat hepatocyte suspensions from 3-month-old male mice (C57BL6-J) were exposed with NPS of varying concentrations, then maintained in Dulbecco's modified eagle medium under standard cell culture conditions for 24 hours.

2.2 | SOD activity and inhibition experiments

Xanthine-xanthine oxidase method was used to determine the activity of SOD at 550 nm. According to the mechanism, kits (Nanjing Jiancheng Bioengineering Institute, China) were purchased to give convenience to the detection. The concentration of NPS were 0, 1, 5, 10, 20, and 30 ($\times 10^{-6}$ mol/L), respectively. All the measurements were carried out at room temperature (298 K) and repeated three times.

2.3 | UV-vis absorption spectra

UV-vis absorption spectra of SOD solution were monitored in the range of 190 to 430 nm with a spectrometer (UV-2450, Shimadzu, Japan). Different concentrations of NPS (0, 1, 5, 10, 20, and 30 [$\times 10^{-6}$ mol/L]) were interacted with SOD for 30 minutes at 298 K and then analyzed by the spectrometer.

2.4 | Circular dichroism spectra

The secondary structure contents of SOD were determined with circular dichroism (CD; J-810, Jasco, Japan) equipped with CDPro software package (http://lamar.colostate.edu/~sreeram/CDPro). Different concentrations of NPS (0, 10, and 30 [$\times 10^{-6}$ mol/L]) were interacted with SOD for 30 minutes and then analyzed by the spectrometer. The scan wavelength, response time, scan rate, and bandwidth were 190 to 260 nm, 1 second, 200 nm/min, and 1 nm, respectively. All the tests were conducted at 298 K with constant nitrogen flush.

2.5 | Fluorescence measurements

Fluorescence spectra with the emission fluorescence intensities at λ_{em} = 290 to 450 nm and excitation fluorescence intensities at λ_{ex} = 280 nm were recorded on a fluorescence spectrophotometer (F-4600, Hitachi, Japan) equipped with a 10-mm quartz cell and a 150-W xenon lamp. The excitation and emission slit width was set at 5 nm. Photo multiplier tube voltage and scan speed were set at 700 V and 1200 nm/min, respectively. Time-resolved fluorescence measurement (λ_{ex} = 278 nm and λ_{em} = 325 nm) was conducted with a FLS920 equipped fluorescence lifetime and steady state spectrometer (Edinburgh, UK). Fluorescence quenching includes static and dynamic quenching, which can be determined with fluorescence lifetime of fluorophore.[22,23] Equation can be used for the determination as follows.[22]

$$\tau_0/\tau = F_0/F, \quad (1)$$

where τ_0, τ, F_0, and F are the fluorescence lifetime of fluorophore and the fluorescence intensity in the absence and presence of NPS (0, 1, 5, and 10 [$\times 10^{-6}$ mol/L]).

2.6 | Determination of MDA levels in cells

The level of oxidative stress in cells can be reflected by the levels of malondialdehide (MDA), which is from the degradation product of lipid peroxidation. Spectrophotometry is used to determine the content of MDA in cells with NPS (0, 1, 5, and 10 [$\times 10^{-6}$ mol/L]) exposure. Mechnism of the method is as follows. Thiobarbituric acid (TBA) is used to react with MDA, then a colored MDA-TBA complex is produced, which can been detected at 532 nm using a spectrophotometer. Lipid peroxidation assay kit (Jiancheng Bioengineering Institute, Nanjing, China) was used to determine the level of MDA in the cell suspensions.

2.7 | DNA damage assay

Comet assay was used to determine DNA damage level of liver cells with NPS (0, 1, 5, and 10 [$\times 10^{-6}$ mol/L]) exposure. The modified procedures were as follows. The comet slides were made with 0.75% NMA, then cells (suspended in 1% LMA) were placed on the slides. Lysis solution (pH = 10) was prepared with 2.5M NaCl, 0.1M Na_2 EDTA, 10mM Tris, 1% Triton X-100, and 10% DMSO to immersed the slides for 2 hours. Next, DNA denaturation in cold electrophoresis buffer was carried out for 20 minutes after washing with ultrapure water. Electrophoresis was then conducted (25 V, 300 mA) for another 20 minutes, followed by washing for three times with BPS solution (pH = 7.4). Then it was stained and analyzed using fluorescence microscope (Eclipse Ti, Nikon, Japan) coupled with charge coupled device (CCD). Camera was used to analyze the slides after staining with propidium iodide (5 mg/L, 15 minutes). The level of DNA damage was determined to analyze the olive tail moment (OTM) of each comet with CASP software. All experimental steps were conducted in dark and at 277 K to prevent secondary DNA damage.

2.8 | Data analysis

Results were presented as the mean of three replicates and reported as means ± standard deviation (SD). Data were analyzed by one-way analysis of variance (ANOVA) with Tukey's multiple comparison test. $P < .05$ was considered as statistically significant.

3 | RESULTS AND DISCUSS

3.1 | Activity analysis

SOD plays a key role for keeping the balance between intrinsic antioxidant defenses and ROS in cell. The change of SOD activity can generally indicate that excessive ROS needs to be eliminated for avoiding oxidative damage.[23,24] As shown in Figure 1, the activity of SOD increases depending on NPS addition, which suggests that the increase of ROS concentration induced the increase of SOD activity to main the balance of intrinsic antioxidant defenses.

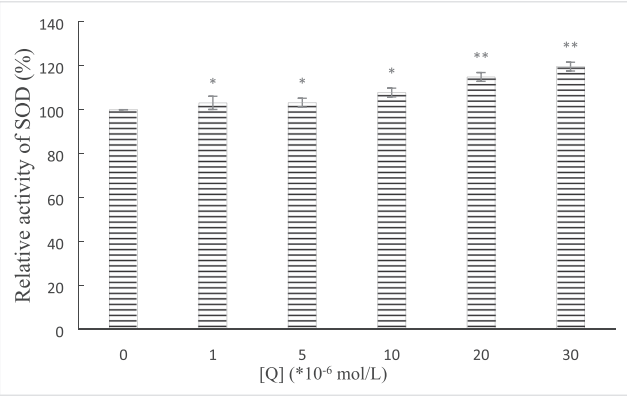

FIGURE 1 Effect of PS on SOD activity. Conditions: NPS ($\times 10^{-6}$ mol/L) 1 to 6: 0, 1, 5, 10, 20, and 30; SOD: 5×10^{-7} mol/L; pH = 7.4; T = 298 K. Statistical significance vs control group: $^*P < .05$, $^{**}P < .01$. The values ± standard deviations were estimated from 60 individual cells in every NPS concentration. NPS, Nanopolystyrene; PS, Polystyrene; SOD, superoxide dismutase

3.2 | Mechanism exploration

This study provides evidence that NPS induced oxidative stress in vitro, but further study is required to clear the mechanism of the current system more precisely.

3.2.1 | Conformational change of SOD investigated by UV-vis

As shown in Figure 2, two main absorption bands of the UV-vis absorption spectroscopy were exhibited, which can reflect the structural change of proteins. The peptide bond π-π* electronic transi-

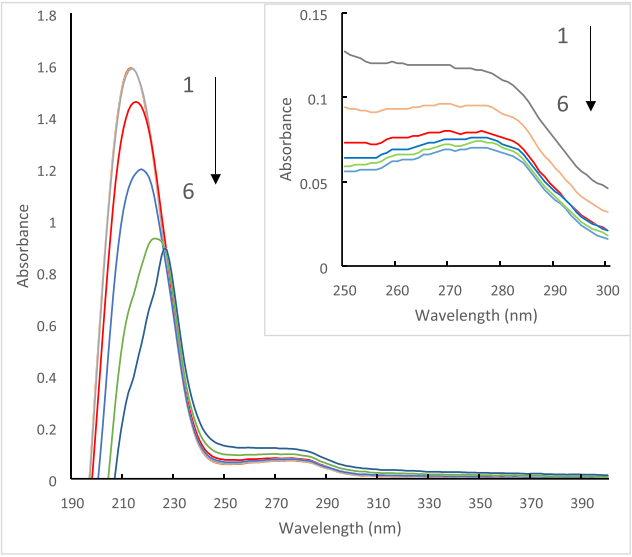

FIGURE 2 UV–vis absorption spectra of SOD in the different concentrations of NPS. The inset is a magnified image around the Soret bands. Conditions: NPS ($\times 10^{-6}$ mol/L) 1 to 6: 0, 1, 5, 10, 20, and 30; SOD: 5×10^{-7} mol/L; pH = 7.4; T = 298 K. NPS, nanopolystyrene; SOD, superoxide dismutase

TABLE 1 Fluorescence lifetime of SOD in different concentrations of NPS

Concentration of NPS ($\times 10^{-6}$ mol/L)	Lifetime, ns	χ^{2a}
0	2.97	1.026
1	2.96	0.933
5	2.95	0.988
10	2.87	0.972

Abbreviations: NPS, nanopolystyrene; SOD, superoxide dismutase.

[a]χ^2 is the reduced chi-square, and a χ^2 value that approaches 1 indicates a perfect fit.

tions of the peptide backbone can be imaged with the strong absorption band at around 209 nm.[25] The weak absorption band (around 280 nm) is involved in the microenvironment of aromatic amino acids (eg, tryptophan and tyrosine).[26,27] The strong peak decreases with concomitant bathochromic shift depending on NPS exposure dose, which represents a hypochromic effect on SOD and the π-π* electronic transition. The weak peak also decreases without red or blue shift, which represents the change of the microenvironment of aromatic amino acids. Considering the increase of SOD activity, this conformational changes of SOD is involved in its activity 1.

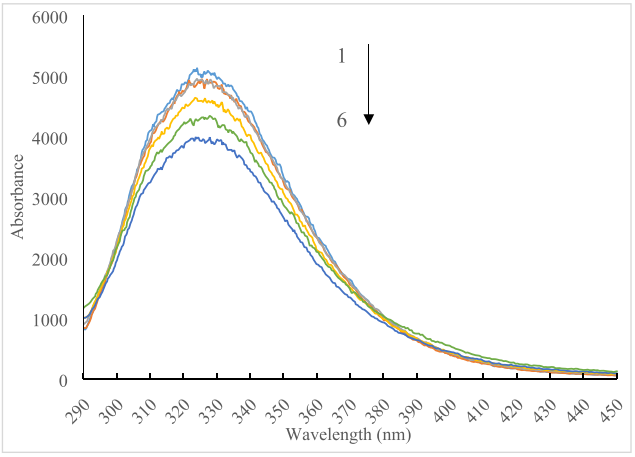

FIGURE 3 Fluorescence emission spectra of SOD in the different concentrations of NPS. λ_{ex} = 280 nm. Conditions: NPS (×10^{-6} mol/L) 1 to 6: 0, 1, 5, 10, 20, and 30; SOD: 5 × 10^{-7} mol/L; pH = 7.4; *T* = 298 K. NPS, nanopolystyrene; SOD, superoxide dismutase

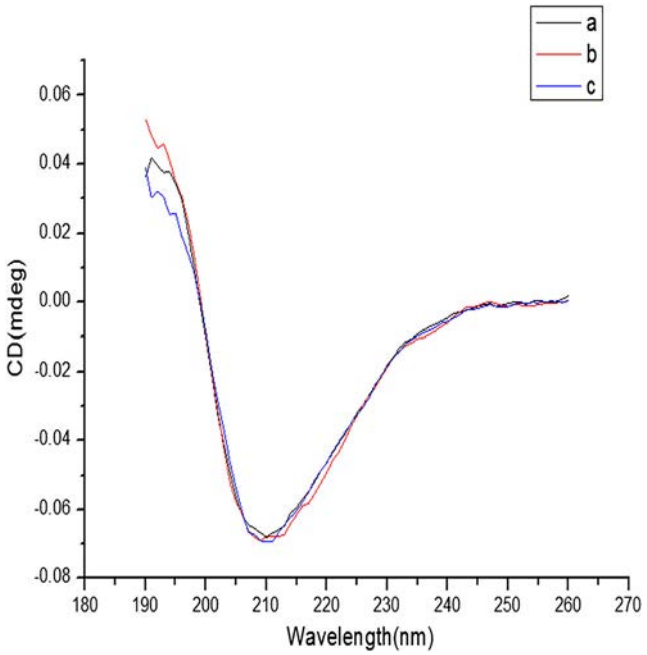

FIGURE 5 Circular dichroism spectrum of SOD in the different concentrations of NPS. Conditions: NPS (×10^{-6} mol/L) a to c: 0, 10, and 30; SOD: 5 × 10^{-7} mol/L; pH = 7.4; *T* = 298 K. NPS, nanopolystyrene; SOD, superoxide dismutase

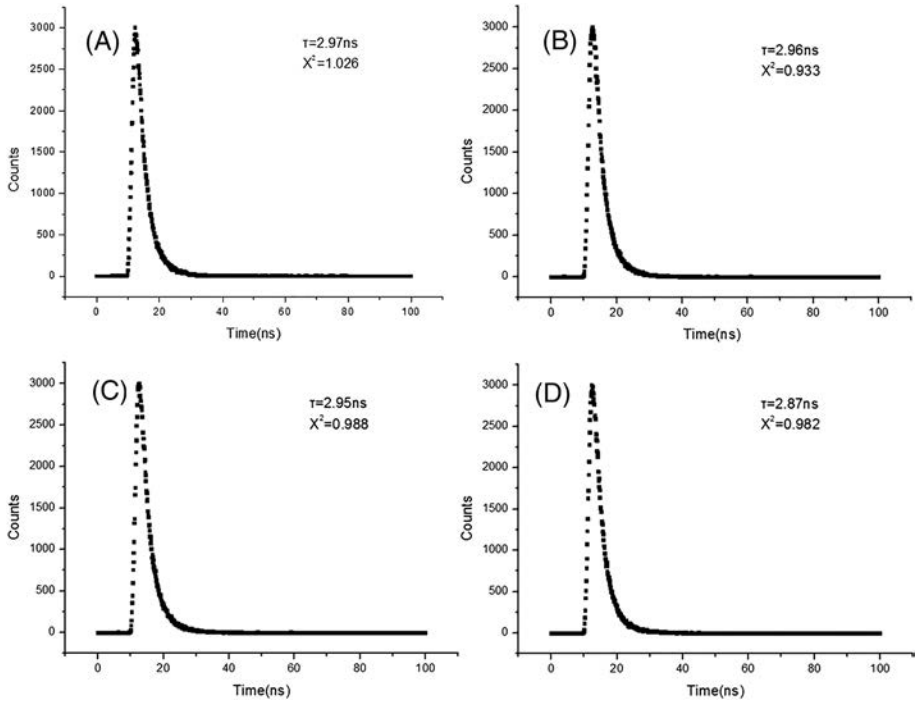

FIGURE 4 Time-resolved fluorescence decay profile of SOD induced by NPS. Conditions: NPS (×10^{-6} mol/L). (A-D) 0, 1, 5, and 10; SOD: 5 × 10^{-7} mol/L; pH = 7.4; *T* = 298 K. NPS, nanopolystyrene; SOD, superoxide dismutase

3.2.2 | Fluorescence quenching of SOD by NPS

The intrinsic fluorescence of SOD is attributed to the aromatic amino acid residues (tryptophan and tyrosine), when the excitation wavelength is set at 280 nm. As shown in Figure 3, the fluorescence emission spectrum of SOD was quenched by NPS exposure. The mechanisms of fluorescence quenching are usually classified into dynamic and static quenching.[28,29] In order to determine the quenching mechanism of SOD caused by NPS exposure, time-resolved fluorescence decay profile was analyzed. The time-resolved decays of SOD with NPS exposure were determined at λ_{ex} = 278 nm and λ_{em} = 325 nm. The data fit well by a single variable monoexponential decay with χ^2 values close to 1.0. As shown in Table 1 and Figure 4, the fluorescence lifetime of SOD shows negligible change with different doses of NPS exposure, which indicates that the quenching mode of SOD fluorescence caused by NPS could be ascribed to the static type.[30]

TABLE 2 Effect of NPS on the percentage of secondary structure content in SOD

Molar Ratio of SOD to PS	Secondary Structure Content in SOD (%)			
	α-Helix	β-Sheet	β-Turns	Unordered
1:0	10.9	39.5	21.9	26.5
1:10	11.5	38.2	20.3	30.2
1:20	17.6	32.4	14.2	29.8

Abbreviations: NPS, nanopolystyrene; PS, polystyrene; SOD, superoxide dismutase.

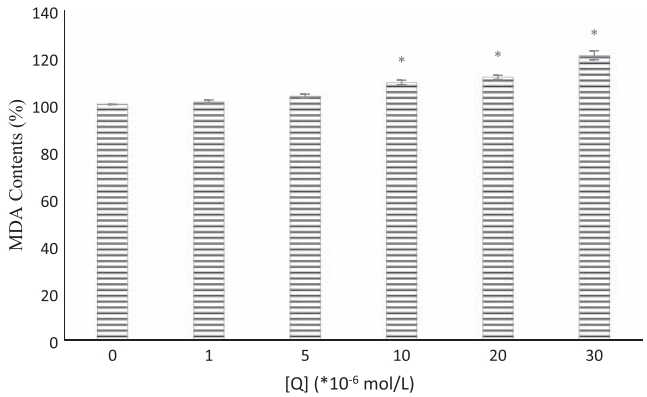

FIGURE 6 Malondialdehyde (MDA) contents in cells in the presence of nanopolystyrene (NPS). Conditions: NPS (×10^{-6} mol/L) 1 to 6: 0, 1, 5, 10, 20, and 30; pH = 7.4; T = 298 K. Statistical significance vs control group: *P < .05. The values ± standard deviations were estimated

3.2.3 | CD spectroscopy

In order to further understand the possible impact of NPS on the conformational changes of SOD, CD is used to investigate the secondary structure change of SOD. As shown in Figure 5, the characteristic negative bands (208 nm) of the α-helix increased in SOD depending on NPS exposure. The contents of four secondary structures of SOD were analyzed with CDPro and listed in Table 2. The content of the α-helix increases from 10.9% to 17.6%. The content of β-fold and β-turn decreases from 39.5% and 21.9% to 32.4% and 14.2%, respectively. This secondary structure change of SOD could lead to the change of physiological function.[31]

3.3 | Analysis of MDA level in cells

The level of MDA, as the main oxidation product of peroxidized polyunsaturated fatty acids, can indicate the degree of lipid peroxidation in the cell. As shown in Figure 6, the level of MDA increases a little with lower exposure concentrations of NPS but increases significantly (P < .05) with higher exposure concentrations of NPS at 1×10^{-5} mol/L. The reason can be that antioxidant defense is resistant to oxidation at low exposure concentrations of NPS, but oxidative stress occurs at high exposure concentrations of NPS. Besides, the change trend of intracellular MDA is consistent with the change of SOD activity, which may be one of the molecular mechanisms involved in the NPS-induced cell toxicity.

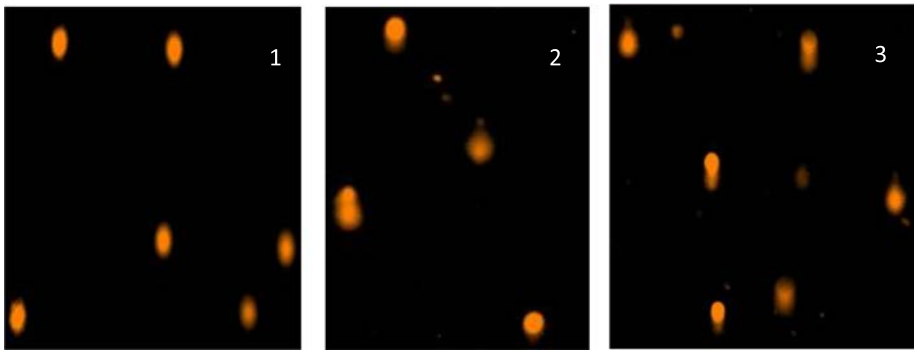

FIGURE 7 Representative images of comet assay after 24-h nanopolystyrene (NPS) treatment. Conditions: NPS (×10^{-6} mol/L) 1 to 3: 0, 1, 5, and 10; pH = 7.4; T = 298 K

TABLE 3 Effect of NPS on DNA damage in mice hepatic cells evaluated by comet assay

Concentration, μM	Tail Length, μm	Tail DNA(%)	Tail Moment	Olive Tail Moment
0	3 ± 0.0000	0.0140 ± 0.0084	0.0005 ± 0.0000	0.0017 ± 0.0010
5	15 ± 0.6667***	21.3620 ± 2.8102**	3.2288 ± 0.5757*	3.8330 ± 0.6183*
10	22 ± 0.6667***	42.1647 ± 6.8672***	9.2274 ± 1.1936***	7.7028 ± 1.6123***

Note. n = 3. Data are expressed as mean ± SD.

*0.01 < P <0.05 by t test, compared with control group.

**0.001 < P <0.01 by t test, compared with control group.

***P <0.001 by t test, compared with control group.

3.4 | NPS induced indirect DNA damage

The degree of DNA damage can be determined with comet assay. Some indicators, such as OTM, head optical density and tail DNA percentage, were widely used to reflect the degree of DNA damage.[32,33] Therefore, comet assay of cells induced by NPS was carried out under alkaline conditions. Comet images of live cells exposed to different concentrations of NPS (0, 5, and 10μM) were shown in Figure 7 and Table 3 (analyzed with CASP software). It is apparent that cells are intact without comet tails for the control group presents, while longer comet tails appear in the experimental groups depending on the exposure concentration of NPS. OTM, head optical density, and tail DNA percentage increase significantly in NPS exposure groups, shown in Table 3. Furthermore, OTM and tail DNA(%) can be the most relevant parameters to probe a dose-dependent DNA damage level compared with tail length and tail moment.[34]

4 | CONCLUSION

The interaction between NPS and SOD induces oxidative stress, involving in the increase of SOD activity and MDA content, and DNA damage. Conformational change of SOD occurs with NPS exposure as revealed by UV-vis absorption and CD spectroscopy studies. The fluorescence quenching of SOD induced by NPS is attributable primarily to resonance energy transfer between fluorophore SOD and NPS. Moreover, comet assay certificated the DNA damage exposed by NPS because of the increase of OTM, head optical density, and tail DNA percentage in exposed groups. This study will help us better understand the human health risks caused by NPS exposure. The methods used in this paper could also be applied to explore the molecular mechanisms of other organic pollutants toxicity.

ACKNOWLEDGEMENTS

This study has been supported by National Natural Science Foundation of China (21507071), Guangzhou Key Laboratory of Environmental Exposure and Health (GDKLEEH201805), Natural Science Foundation of Shandong Province, China (ZR2019BB049), The Fundamental Research Funds of Shandong University (2018JC059), and China Postdoctoral Science Foundation funded project (2018M640631).

CONFLICT OF INTEREST

All authors (C.L., T.Z., and D.Y.) declare that they have no known competing financial interests or personal relationships that could have appeared to influence the work reported in this paper.

AUTHOR CONTRIBUTIONS

Tongtong Zheng (T.Z.) performed the research. Chunguang Liu (C.L.) designed the research study. C.L. and Dong Yuan (D.Y.) contributed essential reagents or tools. T.Z., and C. L analyzed the data. T.Z., D. Y., and C.L. wrote the paper.

ORCID

Chunguang Liu https://orcid.org/0000-0003-1635-4260

REFERENCES

1. Cole M, Lindeque P, Halsband C, Galloway TS. Microplastics as contaminants in the marine environment: a review. *Mar Pollut Bull*. 2011;62(12):2588-2597.
2. Murphy F, Ewins C, Carbonnier F, Quinn B. Wastewater treatment works (WwTW) as a source of microplastics in the aquatic environment. *Environ Sci Technol*. 2016;50(11):5800-5808.
3. Blasco J, Corsi I, Matranga V. Particles in the oceans: implication for a safe marine environment. *Mar Environ Res*. 2015;111(Supplement C):1-4.
4. Jeong C-B, Kang H-M, Lee M-C, et al. Adverse effects of microplastics and oxidative stress-induced MAPK/Nrf2 pathway-mediated defense mechanisms in the marine copepod Paracyclopina nana. *Sci Rep*. 2017;7(1):41323.
5. Gewert B, Ogonowski M, Barth A, MacLeod M. Abundance and composition of near surface microplastics and plastic debris in the Stockholm Archipelago, Baltic Sea. *Mar Pollut Bull*. 2017;120(1):292-302.
6. Nobre CR, Santana MFM, Maluf A, et al. Assessment of microplastic toxicity to embryonic development of the sea urchin *Lytechinus variegatus* (Echinodermata: Echinoidea). *Mar Pollut Bull*. 2015;92(1):99-104.
7. Fisner M, Taniguchi S, Majer AP, Bícego MC, Turra A. Concentration and composition of polycyclic aromatic hydrocarbons (PAHs) in plastic pellets: implications for small-scale diagnostic and environmental monitoring. *Mar Pollut Bull*. 2013;76(1):349-354.
8. Zitting A, Heinonen T, Vainio H. Glutathione depletion in isolated rat hepatocytes caused by styrene and the thermal degradation products of polystyrene. *Chem Biol Interact*. 1980;31(3):313-318.

9. Jeong C-B, Won E-J, Kang H-M, et al. Microplastic size-dependent toxicity, oxidative stress induction, and p-JNK and p-p38 activation in the monogonont rotifer (*Brachionus koreanus*). *Environ Sci Technol*. 2016;50(16):8849-8857.
10. Corsi I, Cherr GN, Lenihan HS, et al. Common strategies and technologies for the ecosafety assessment and design of nanomaterials entering the marine environment. *ACS Nano*. 2014;8(10):9694-9709.
11. Canesi L, Ciacci C, Bergami E, et al. Evidence for immunomodulation and apoptotic processes induced by cationic polystyrene nanoparticles in the hemocytes of the marine bivalve *Mytilus*. *Mar Environ Res*. 2015;111:34-40.
12. Fleischer CC, Payne CK. Nanoparticle–cell interactions: molecular structure of the protein corona and cellular outcomes. *Acc Chem Res*. 2014;47(8):2651-2659.
13. She Y, Jiang L, Zheng L, et al. The role of oxidative stress in DNA damage in pancreatic β cells induced by di-(2-ethylhexyl) phthalate. *Chem Biol Interact*. 2017;265:8-15.
14. Lu Y, Zhang Y, Deng Y, et al. Uptake and accumulation of polystyrene microplastics in zebrafish (*Danio rerio*) and toxic effects in liver. *Environ Sci Technol*. 2016;50(7):4054-4060.
15. von Moos N, Burkhardt-Holm P, Köhler A. Uptake and effects of microplastics on cells and tissue of the blue mussel *Mytilus edulis* L. after an experimental exposure. *Environ Sci Technol*. 2012;46(20):11327-11335.
16. Manke A, Wang L, Rojanasakul Y. Mechanisms of nanoparticle-induced oxidative stress and toxicity. *Biomed Res Int*. 2013;2013:15.
17. Pan X, Qin P, Liu R, Yu W, Dong X. Effects of carbon chain length on the perfluoroalkyl acids-induced oxidative stress of erythrocytes in vitro. *J Agric Food Chem*. 2018;66(25):6414-6420.
18. Lushchak VI. Environmentally induced oxidative stress in aquatic animals. *Aquat Toxicol*. 2011;101(1):13-30.
19. Nasser F, Lynch I. Secreted protein eco-corona mediates uptake and impacts of polystyrene nanoparticles on *Daphnia magna*. *J Proteomics*. 2016;137:45-51.
20. Galloway TS. Micro- and nano-plastics and human health. In: Bergmann M, Gutow L, Klages M, eds. *Marine Anthropogenic Litter*. Cham: Springer International Publishing; 2015:343-366.
21. Fröhlich E. The role of surface charge in cellular uptake and cytotoxicity of medical nanoparticles. *Int J Nanomedicine*. 2012;7:5577-5591.
22. Lakowicz JR. Quenching of fluorescence. In: *Principles of Fluorescence Spectroscopy*. Boston, MA: Springer US; 1999:237-265.
23. Wang J, Zhang H, Zhang T, Zhang R, Liu R, Chen Y. Molecular mechanism on cadmium-induced activity changes of catalase and superoxide dismutase. *Int J Biol Macromol*. 2015;77:59-67.
24. Hao M, Liu R. Conformational and functional effects of MPA-CdTe quantum dots on SOD: evaluating the mechanism of oxidative stress induced by quantum dots in the mouse nephrocytes. *J Mol Recognit*. e2783.
25. Scopes RK. Measurement of protein by spectrophotometry at 205 nm. *Anal Biochem*. 1974;59(1):277-282.
26. Mansur HS, Lobato ZP, Oréfice RL, Vasconcelos WL, Oliveira C, Machado LJ. Surface functionalization of porous glass networks: effects on bovine serum albumin and porcine insulin immobilization. *Biomacromolecules*. 2000;1(4):789-797.
27. Yang B, Hao F, Li J, Chen D, Liu R. Binding of chrysoidine to catalase: spectroscopy, isothermal titration calorimetry and molecular docking studies. *J Photochem Photobiol B Biol*. 2013;128(Supplement C):35-42.
28. Hu Y-J, Yue H-L, Li X-L, Zhang S-S, Tang E, Zhang L-P. Molecular spectroscopic studies on the interaction of morin with bovine serum albumin. *J Photochem Photobiol B Biol*. 2012;112(Supplement C):16-22.
29. Das S, Islam MM, Jana GC, Patra A, Jha PK, Hossain M. Molecular binding of toxic phenothiazinium derivatives, azures to bovine serum albumin: a comparative spectroscopic, calorimetric, and in silico study. *J Mol Recognit*. 2017;30(7):e2609.
30. Zhang H, Liu Y, Liu R, Liu C, Chen Y. Molecular mechanism of lead-induced superoxide dismutase inactivation in zebrafish livers. *J Phys Chem B*. 2014;118(51):14820-14826.
31. Koshland DE. Correlation of structure and function in enzyme action. *Science*. 1963;142(3599):1533-1541.
32. Dar AM, Ishrat U, Yaseen Z, Shamsuzzaman, Gatoo MA. In vitro cytotoxcity and interaction of new steroidal oxadiazinanones with calf thymus DNA using molecular docking, gel electrophoresis and spectroscopic techniques. *J Photochem Photobiol B Biol*. 2015;148(Supplement C):340-350.
33. Ahmad L, Jalali S, Shami SA, Akram Z, Batool S, Kalsoom O. Effects of cryopreservation on sperm DNA integrity in normospermic and four categories of infertile males. *Syst Biol Reprod Med*. 2010;56(1):74-83.
34. Zhang H, Wei K, Zhang M, Liu R, Chen Y. Assessing the mechanism of DNA damage induced by lead through direct and indirect interactions. *J Photochem Photobiol B Biol*. 2014;136(Supplement C):46-53.

How to cite this article: Zheng T, Yuan D, Liu C. Molecular toxicity of nanoplastics involving in oxidative stress and desoxyribonucleic acid damage. *J Mol Recognit*. 2019;32:e2804. https://doi.org/10.1002/jmr.2804